

RESEARCH ARTICLE

10.1002/2014JG002715

Key Points:

- Ten year OC burial and accretion rates are greater than 100 year rates
- Spatial variability of these rates decreases over the same timescales
- OC is an important soil-building component in the coastal Everglades

Supporting Information:

- Readme
- Table S1

Correspondence to:

J. L. Breithaupt,
jlbreith@mail.usf.edu

Citation:

Breithaupt, J. L., J. M. Smoak, T. J. Smith III, and C. J. Sanders (2014), Temporal variability of carbon and nutrient burial, sediment accretion, and mass accumulation over the past century in a carbonate platform mangrove forest of the Florida Everglades, *J. Geophys. Res. Biogeosci.*, 119, doi:10.1002/2014JG002715.

Received 29 MAY 2014

Accepted 27 SEP 2014

Accepted article online 1 OCT 2014

Temporal variability of carbon and nutrient burial, sediment accretion, and mass accumulation over the past century in a carbonate platform mangrove forest of the Florida Everglades

Joshua L. Breithaupt¹, Joseph M. Smoak², Thomas J. Smith III³, and Christian J. Sanders⁴

¹College of Marine Science, University of South Florida, St. Petersburg, Florida, USA, ²Department of Environmental Science, Policy, and Geography, University of South Florida, St. Petersburg, Florida, USA, ³U.S. Geological Survey, Southeast Ecological Science Center, St. Petersburg, Florida, USA, ⁴Centre for Coastal Biogeochemistry Research, School of Environment, Science & Engineering, Southern Cross University, Lismore, New South Wales, Australia

Abstract The objective of this research was to measure temporal variability in accretion and mass sedimentation rates (including organic carbon (OC), total nitrogen (TN), and total phosphorous (TP)) from the past century in a mangrove forest on the Shark River in Everglades National Park, USA. The ²¹⁰Pb Constant Rate of Supply model was applied to six soil cores to calculate annual rates over the most recent 10, 50, and 100 year time spans. Our results show that rates integrated over longer timeframes are lower than those for shorter, recent periods of observation. Additionally, the substantial spatial variability between cores over the 10 year period is diminished over the 100 year record, raising two important implications. First, a multiple-decade assessment of soil accretion and OC burial provides a more conservative estimate and is likely to be most relevant for forecasting these rates relative to long-term processes of sea level rise and climate change mitigation. Second, a small number of sampling locations are better able to account for spatial variability over the longer periods than for the shorter periods. The site average 100 year OC burial rate, 123 ± 19 (standard deviation) $\text{g m}^{-2} \text{yr}^{-1}$, is low compared with global mangrove values. High TN and TP burial rates in recent decades may lead to increased soil carbon remineralization, contributing to the low carbon burial rates. Finally, the strong correlation between OC burial and accretion across this site signals the substantial contribution of OC to soil building in addition to the ecosystem service of CO₂ sequestration.

1. Introduction

Although mangroves only cover between 138,000 and 152,000 km² [Giri *et al.*, 2011; Spalding *et al.*, 2010], these forested wetlands are of great value for their contributions to environmental, societal, and economic functions around the globe. In addition to providing habitat for numerous fauna and supporting food webs (directly and indirectly) [Bui and Lee, 2014; Kristensen *et al.*, 2008; Nagelkerken *et al.*, 2008], natural resources for human communities [Walters *et al.*, 2008] along with stabilization and protection of shorelines from tsunamis and storm surge [Alongi *et al.*, 2008; Costanza *et al.*, 2008], these wetlands make a substantial contribution to the global carbon budget [Bouillon *et al.*, 2008; Breithaupt *et al.*, 2012; Dittmar *et al.*, 2006; Donato *et al.*, 2011; Duarte *et al.*, 2005; Jennerjahn and Ittekkot, 2002; Mcleod *et al.*, 2011]. When looking specifically at the soil component of the budget, the quantitative research can be broadly categorized according to whether the focus is the organic carbon (OC) standing stock [Adame *et al.*, 2013; Donato *et al.*, 2011, 2012; Kauffman *et al.*, 2011] or the rate of OC burial [Breithaupt *et al.*, 2012, and references therein; Chmura *et al.*, 2003; Mcleod *et al.*, 2011].

Understanding of the OC stock and burial rates further informs research that quantitatively estimates the global impact to atmospheric CO₂ levels from projected mangrove deforestation and peat loss, or conversely the offset potential that may be achieved through mangrove conservation [Alongi, 2011; Pendleton *et al.*, 2012; Siikamäki *et al.*, 2012; Ullman *et al.*, 2012]. An increasing number of studies have utilized ²¹⁰Pb as a tracer of the net OC accumulation rate in mangrove soils across a centennial time span in order to assess the response of these systems to recent sea level rise as well as accounting for their capacity to sequester atmospheric CO₂ on a timescale of relevance to anthropogenic climate change [Alongi *et al.*, 2001, 2004; Brunskill *et al.*, 2004; Sanders *et al.*, 2012; Smoak *et al.*, 2013]. Additionally, understanding the factors that

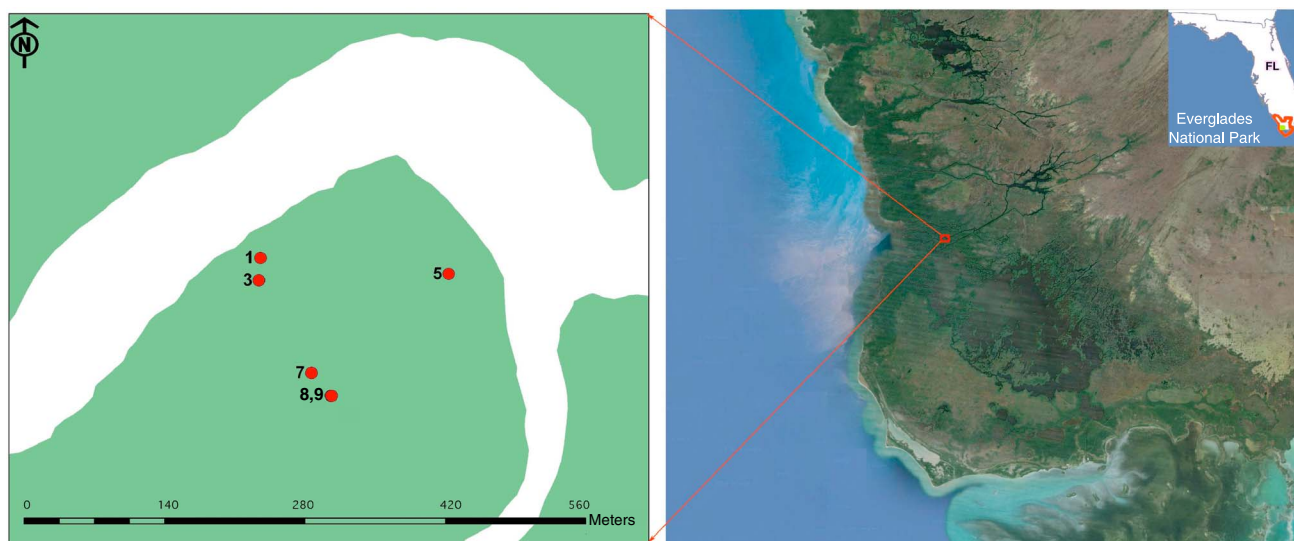


Figure 1. (right) Site location on Shark River in southwestern Everglades National Park, FL, USA. (left) Locations of soil cores (25°21'50"N 81°4'42"W). Cores are the following distances from a main creek: SH3-1: 25 m; SH3-3: 35 m; SH3-5: 50 m; SH3-7: 145 m; SH3-8: 170 m; and SH3-9: 171 m. Note that cores SH3-8 and SH3-9 were collected 1 m apart and are represented as a single point on the figure.

control OC burial rate variability can help planners to estimate the time it might take for a restored or newly planted mangrove wetland to accumulate a target stock of soil carbon.

The most recent review of centennial-timescale carbon burial rates concluded that mangroves bury a mean rate of $163 \text{ g OC m}^{-2} \text{ yr}^{-1}$ at the local level, or 26.1 Tg yr^{-1} globally [Breithaupt et al., 2012]. That assessment identified substantial gaps in global sampling coverage as well as a need for better explanation of the control mechanisms contributing to the wide range of burial rates. These control mechanisms include latitudinal position, the amount and type of sediment supply, nutrient availability, intertidal position, and the frequency and intensity of storm occurrences.

The objective of our research was to provide an estimate for rates of accretion and mass sedimentation (including OC, total nitrogen (TN), and total phosphorous (TP)) in the mangroves of the southwestern Everglades. Pb-210 was used to date soil cores collected within a relatively small spatial footprint ($<200 \text{ m}$), accounting for 10, 50, and 100 year timescales. Our first hypothesis was that accretion and mass sedimentation rates would be higher for the short-term record and lower over longer periods of observation based on assumptions of ongoing organic matter degradation and recent storm surge deposition [Smoak et al., 2013]. Second, based on high productivity [Barr et al., 2010, 2011; Simard et al., 2006], and high soil OC% [Castañeda-Moya et al., 2011; Chen and Twilley, 1999a], we hypothesized that the mean OC burial rate in this forest exceeds the global average for mangroves.

2. Methods

2.1. Study Site

The study site is an estuarine mangrove forest approximately 4 km inland from the Gulf of Mexico on the Shark River in Everglades National Park (Figure 1). The mangrove species present are red (*Rhizophora mangle*), black (*Avicennia germinans*), and white (*Laguncularia racemosa*), with a canopy height of approximately 13 to 19 m [Krauss et al., 2006; Whelan et al., 2009], mean stem density of 2838 ha^{-1} , and basal area of $40.9 \text{ m}^2 \text{ ha}^{-1}$ [Castañeda-Moya et al., 2013]. Net Primary Productivity (aboveground and belowground) is $1920 \text{ g m}^{-2} \text{ yr}^{-1}$ [Castañeda-Moya et al., 2013]. The average soil surface is approximately 0.2 m above mean sea level and average pore water salinity is 24.6 ± 2.4 [Krauss et al., 2006]. Several elevation lows in the form of tidal rivulets within the forest are present in the area where cores were collected. Local tides are semidiurnal with an average amplitude ranging from 0.5 to 1.0 m, and much of the site is completely inundated twice a day [Barr et al., 2010; Romigh et al., 2006]. The soil at the site is composed of 5.5 m of peat above the limestone bedrock [Whelan et al., 2005] and is indicative of a system whose soil

accumulation is due primarily to autochthonous sources of organic matter detritus rather than deposition of terrigenous mineral sediments. The lack of substantial terrigenous input via the upstream freshwater flow is accompanied by a similar limitation in phosphorous (P), the primary limiting nutrient to macrophyte growth, including mangroves, in the Everglades [Childers *et al.*, 2006; Noe *et al.*, 2001]. This limitation is countered by provision of P from the Gulf of Mexico [Chen and Twilley, 1999b; Fourqurean *et al.*, 1992], leading to the description of the coastal Everglades as an “upside down estuary” [Childers *et al.*, 2006] with the highest productivity found in the belt of mangroves along the southwestern extent where this research was conducted [Simard *et al.*, 2006].

This region of South Florida has been impacted by at least four major hurricanes since 1929, each influencing the nature of forest and soil characteristics [Smith *et al.*, 1994, 2009]. Most recently, Hurricane Wilma passed just north of the site in 2005, and deposited 37 (± 3.0 SE) mm of fine-grained marine carbonate sediment [Whelan *et al.*, 2009]. This layer was shown to have a high concentration of TP (0.36 ± 0.02 mg cm⁻³) compared to prestorm soils (0.22 ± 0.02 mg cm⁻³) [Castañeda-Moya *et al.*, 2010]. Smoak *et al.* [2013], working with core SH3-1 from this data and a second core approximately 9.5 km from the mouth of the Harney River, found that soil mass accumulation, surface accretion, and OC burial rates were all elevated in this Wilma layer.

2.2. Soil Sampling and Processing

A Russian peat corer was used to collect six 50 cm deep soil cores from within 200 m of each other at a single site near the main creek of the Shark River (Figure 1). Similar core numbers have been utilized to study spatial variability over scales of hundreds to thousands of meters in mangrove environments around the globe [Breithaupt *et al.*, 2012, and references therein]. SH3-1 was retrieved in February and SH3-3 in December of 2009. The remaining four cores were collected in November of 2010. Each core was sectioned in 1 cm intervals, with the exception of SH3-1, which was sectioned in 2 cm intervals beginning at 10 cm depth. An aliquot was taken from each interval for gravimetric analyses of wet weight, dry weight, and loss-on-ignition weight (LOI). Dry weight was obtained by drying at 105°C for 24 h, and LOI was obtained by heating in a muffle furnace at 550°C for 1 h. Hereafter, Organic Matter (OM) refers to the material lost via LOI, and Inorganic Matter (IM) refers to the remaining material. Soil density was calculated as aliquot dry mass divided by initial wet volume.

2.3. C, N, Stable Isotopes ($\delta^{13}\text{C}$ and $\delta^{15}\text{N}$), and TP

Soil from each interval was analyzed for TOC, TN, $\delta^{13}\text{C}$, and $\delta^{15}\text{N}$. Samples were acidified to remove carbonate material prior to analysis and were processed using a PDZ Europa ANCA-GL (Automated Nitrogen Carbon Analyzer-Gas Solids Liquids) elemental analyzer connected to a PDZ Europa 20-20 isotope ratio mass spectrometer. The average relative standard deviation based on duplicate samples from the two cores was 0.28% for C and 0.02% for N. For analytical precision of stable isotopes, the instrumentation error is expected to be less than 0.2‰ for $\delta^{13}\text{C}$ and 0.3‰ for $\delta^{15}\text{N}$ based on long-term standard deviations of samples compared to standards.

The analysis of TP was conducted using a Perkin Elmer ELAN DRc ICPMS (Dynamic Reaction Cell-equipped Inductively-Coupled Plasma Mass Spectrometer). The Laboratory Control Sample (LCS) was AGAL 12, which was digested and analyzed as part of each batch. Duplicates were done every 10 samples. The calibration curve was 0.1, 1, 10, and 100 ppm phosphorus generating an R^2 greater than 0.9999.

2.4. Core Dating and Rate Calculation

Soil accumulation rates were determined using excess ^{210}Pb ($^{210}\text{Pb}_{\text{ex}}$), a radionuclide with a half-life of 22.3 years and well suited to the timescale of interest here (≤ 100 years). Measurements and calculations were conducted as described by Smoak *et al.* [2013]. Briefly, sectioned core intervals were freeze dried, homogenized, and packed in gamma counting tubes. Gamma activities were measured using an intrinsic germanium well detector coupled to a multichannel analyzer. Activity for ^{210}Pb was measured by the 46.5 keV peak and ^{226}Ra by using its proxy ^{214}Pb (351.9 keV peak) [Appleby *et al.*, 1988]. Because the study site has been subject to hurricane activity and the storm surge that accompanies such events can be a source of significant marine sediment deposition, the sediment accumulation rate has been calculated following the Constant Rate of Supply (CRS) model. This model is intended for use in systems in which the initial concentration of unsupported ^{210}Pb is periodically diluted by an increase in local production or an addition

Table 1. Mean and Standard Deviation (SD) of Soil Characteristics From Dated Intervals (~ ≤ 100 yrs)^a

Core	Bulk Density (g cm ⁻³)		Organic Matter (%)		Organic C (%)		Organic C (mg cm ⁻³)		Total N (mg cm ⁻³)		Total P (mg cm ⁻³)		Atomic C:N		Atomic N:P		δ ¹³ C (‰)		δ ¹⁵ N (‰)	
	Mean	SD	Mean	SD	Mean	SD	Mean	SD	Mean	SD	Mean	SD	Mean	SD	Mean	SD	Mean	SD	Mean	SD
SH3-1	0.28	0.18	43%	13%	19%	6%	43.8	9.2	3.0	1.7	0.23	0.04	19.3	4.0	29.6	18.4	-27.5	0.6	3.4	0.8
SH3-3	0.21	0.05	40%	6%	18%	2%	37.9	5.7	2.5	0.4	0.26	0.04	18.1	1.7	21.0	2.6	-26.1	0.8	3.2	0.4
SH3-5	0.17	0.05	59%	9%	27%	3%	45.0	10.6	2.6	0.9	0.22	0.06	19.1	1.0	27.5	2.8	-26.6	0.3	2.8	0.2
SH3-7	0.21	0.09	54%	12%	26%	7%	51.9	9.2	2.5	0.4	0.19	0.06	24.7	2.2	29.6	5.7	-26.0	1.1	3.1	0.3
SH3-8	0.21	0.08	57%	12%	25%	6%	49.1	10.3	2.2	0.7	0.19	0.06	23.3	2.4	27.8	4.6	-25.8	0.8	3.0	0.3
SH3-9	0.16	0.03	56%	12%	27%	4%	41.2	7.6	2.1	0.5	0.15	0.03	23.0	2.0	30.8	5.7	-26.4	0.9	3.2	0.4
Site	0.20	0.09	52%	12%	24%	6%	44.9	10.0	2.5	0.9	0.21	0.06	21.2	3.4	27.6	8.5	-26.4	0.9	3.1	0.5

^aBold font values are the mean and standard deviation for all six cores.

of allochthonous material without excess ²¹⁰Pb [Appleby and Oldfield, 1978]. Although often used to corroborate ²¹⁰Pb_{ex} dates, there were no distinct ¹³⁷Cs peaks detected in these cores; this is likely due to ¹³⁷Cs being highly mobile in organic soils that lack clays. This lack of independent corroboration of the dates adds to the uncertainty of the model-calculated ages.

Dates derived for the bottom of each sectioned soil interval enable the calculation of the rates used in this study:

1. Mass accumulation rate = interval mass (g m⁻²)/# of years in the interval.
2. Soil accretion rate = density-corrected interval depth (mm)/# of years in the interval.

The accumulation rates of inorganic matter (IM), organic matter (OM), organic carbon (OC), total nitrogen (TN), and total phosphorous (TP) are each calculated as their respective percentages of the total mass accumulation rate for each interval.

Surface accretion corresponds to increased mass, which has a compacting effect on the underlying layers. Therefore, the interval depths of lower bulk density have been normalized to the density of the bottom layers to account for this autocompaction [Lynch et al., 1989].

2.5. Decadal Aggregation of Site Mean Rates

The CRS model attributes dates to each sectioned soil-depth interval; however, the model dates are frequently different for corresponding depth intervals of different cores because of varying soil accumulation rates. In order to make site-wide time interval measurements the cores need to be standardized to common age intervals (rather than depth intervals). Decadal years (e.g., 1980, 1990, and 2000) were used as interval boundaries and were considered as a fraction of the respective interval's age. Using a hypothetical example, take the CRS-modeled date for the bottom of an interval as 1998 and the date at the top of the interval as 2005. Assuming a constant sediment accumulation rate within the interval, the decadal break at the year 2000 occurs at 29% of the interval's total age. Consequently, 29% of the interval's mass and volume is assigned to the decade from 1990 to 1999, and the remaining 71% is assigned to the decade that occurred from 2000 to 2009. The annual rate for each decade is then calculated as the sum of the mass within the decade divided by 10 years.

3. Results

3.1. Soil Bulk Density, Organic Matter, TOC, TN, TP, δ¹³C, and δ¹⁵N

The mean dry bulk density (DBD) for all intervals is 0.20 ± 0.09 (standard deviation) g cm⁻³ (Table 1). The mean OM percentage for all intervals is 52 ± 12. Overall, DBD is highest in the first 7 cm (0.29 ± 0.16 g cm⁻³) before becoming relatively uniform throughout intervals 8–40 cm (0.18 ± 0.04 g cm⁻³) (Figure 2). The pattern for OM percentage is opposite, with lower values in the top 7 cm (40 ± 15%) and higher, more uniform values over the remaining depths (55 ± 8%).

The mean total OC for the dated intervals of all six cores was 24 ± 6% or 44.9 ± 10.0 mg cm⁻³ (Table 1). The mean TN was 2.5 ± 0.9 mg cm⁻³, and TP was 0.21 ± 0.06 mg cm⁻³. Molar C:N for these bulk sediments was 21.2 ± 3.4, and N:P was 27.6 ± 8.5.

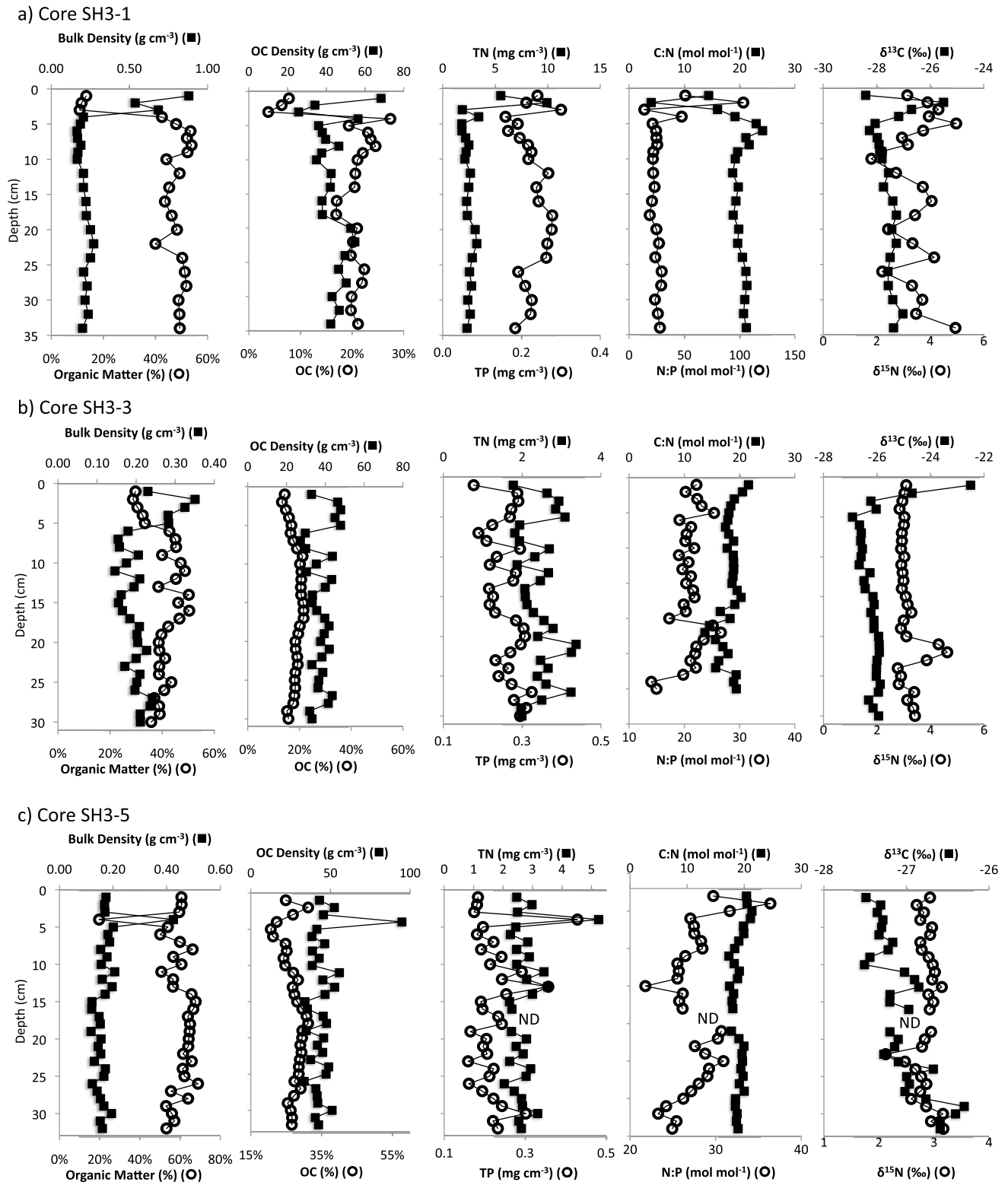
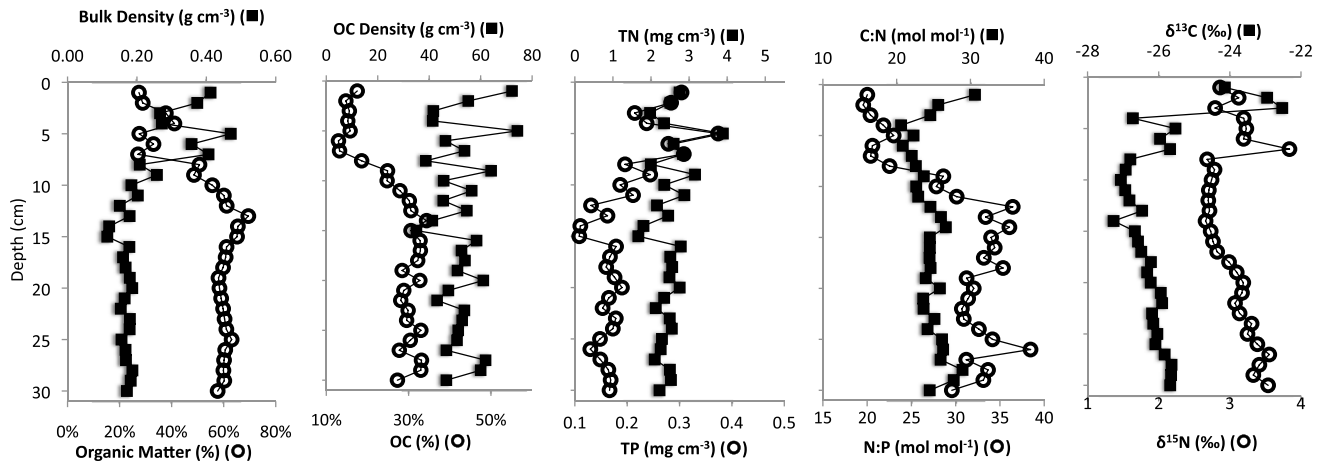
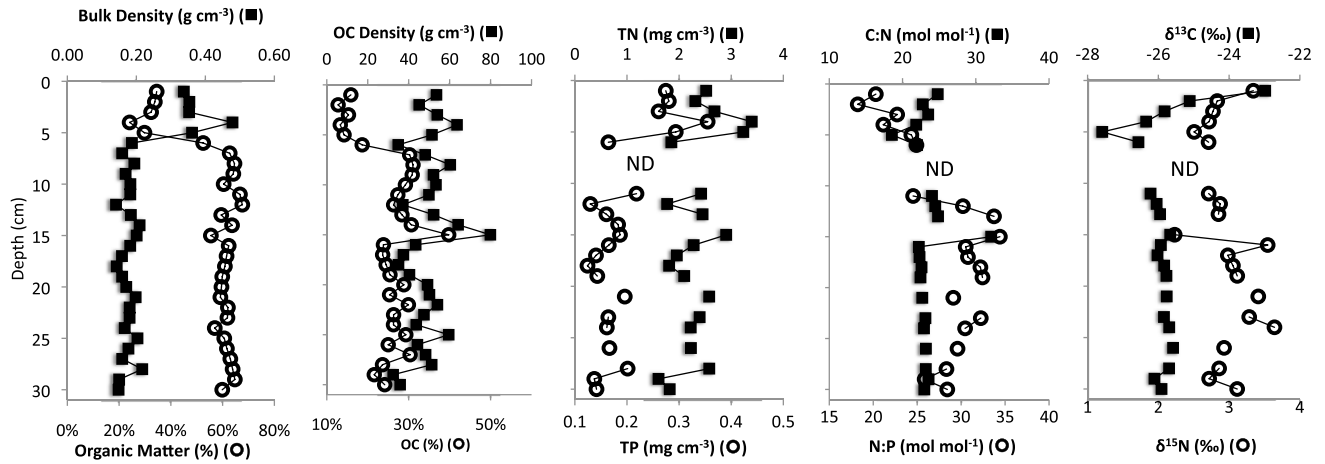


Figure 2. (a–f) Depth profiles of soil characteristics for dated intervals (≤ 100 years) of the six soil cores. Data gaps (ND) in cores SH3-5 and SH3-8 are due to lack of available sediment for analysis (continued on next page).

d) Core SH3-7



e) Core SH3-8



f) Core SH3-9

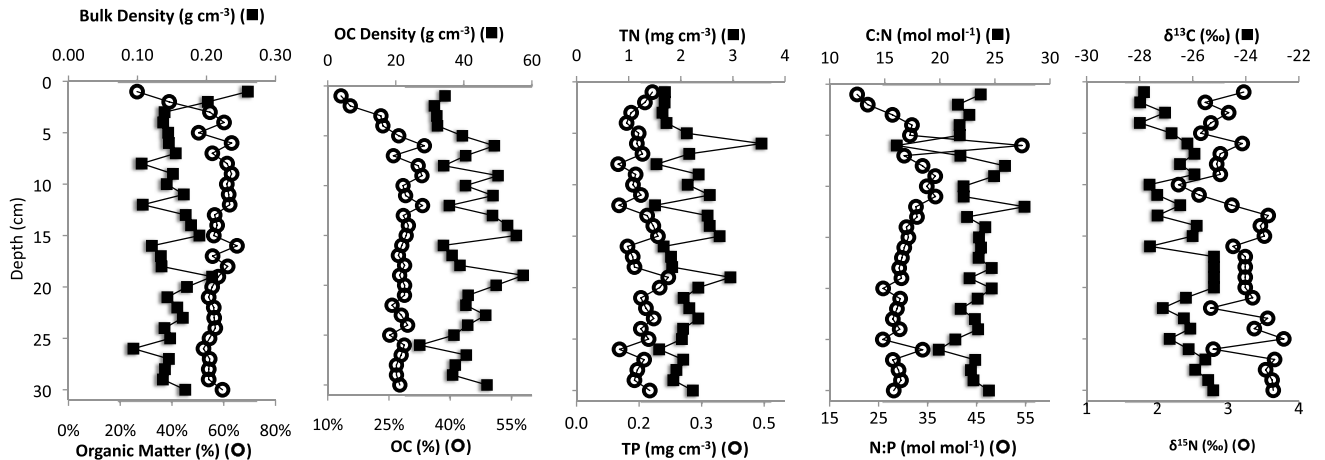


Figure 2. (continued)

Table 2. Excess ^{210}Pb Activity (dpm g^{-1}), CRS Model Age at Bottom of Each Interval (Years), and 1 Standard Age Error (Years) for Soil Cores^a

Depth Interval	SH3-1			SH3-3			SH3-5			SH3-7			SH3-8			SH3-9		
	$^{210}\text{Pb}_{\text{XS}}$	Age	Age Error															
0-1	1.9	2.6	0.5	3.7	1.5	0.7	4.7	1.0	0.6	4.4	2.8	1.5	4.1	2.0	0.6	4.4	2.1	0.6
1-2	1.0	3.5	0.5	4.4	4.4	0.7	5.0	2.2	0.6	4.1	5.3	1.6	3.8	4.1	0.6	4.3	3.7	0.6
2-3	1.0	4.6	0.6	3.9	6.9	0.7	5.2	3.4	0.6	4.3	7.4	1.6	3.9	6.4	0.6	7.6	5.9	0.7
3-4	4.4	6.2	0.6	4.4	9.7	0.7	4.2	5.9	0.7	4.7	9.8	1.7	4.3	10.2	0.6	7.4	8.1	0.7
4-5	6.2	8.4	0.6	3.6	12.1	0.8	4.4	7.3	0.7	4.9	14.8	1.8	4.4	13.4	0.7	6.8	10.4	0.7
5-6	5.7	10.3	0.6	3.9	13.8	0.8	7.1	9.4	0.7	4.3	18.5	2.0	4.1	15.1	0.7	7.2	13.0	0.8
6-7	6.6	12.7	0.6	5.6	16.1	0.8	5.4	11.1	0.7	4.2	23.3	2.2	6.1	17.4	0.7	7.3	16.1	0.8
7-8	4.4	14.6	0.7	4.7	18.3	0.9	5.1	12.6	0.7	4.4	26.2	2.3	5.5	20.1	0.7	7.0	18.3	0.9
8-9	5.3	16.9	0.7	4.4	21.1	0.9	5.3	14.3	0.8	4.9	30.6	2.6	4.2	22.1	0.8	6.3	21.4	0.9
9-10	3.4	18.3	0.7	4.4	23.7	1.0	5.0	15.9	0.8	4.8	34.2	2.8	3.8	24.1	0.8	5.3	24.1	1.0
10-11	4.5	22.2	0.8	3.1	25.4	1.0	5.6	18.4	0.8	4.3	38.1	3.0	3.7	26.2	0.8	4.2	26.8	1.0
11-12				3.4	28.1	1.0	5.4	20.3	0.8	5.5	42.3	3.3	4.4	28.3	0.9	3.3	28.3	1.0
12-13	2.9	24.9	0.9	3.7	31.2	1.1	4.1	22.3	0.8	5.0	47.6	3.7	4.3	31.1	0.9	3.5	30.9	1.1
13-14				3.6	33.9	1.2	4.2	24.2	0.9	2.9	49.9	3.9	3.7	34.1	1.0	2.7	33.2	1.1
14-15	2.8	28.0	0.9	3.5	36.7	1.2	4.5	25.7	0.9	3.0	52.4	4.1	3.4	37.0	1.0	3.0	36.1	1.1
15-16				3.3	39.7	1.3	4.3	27.1	0.9	3.0	56.7	4.4	3.3	39.8	1.1	3.0	38.1	1.2
16-17	2.6	33.1	1.0	3.1	43.2	1.4	4.4	29.1	1.0	3.6	61.9	5.0	3.2	42.4	1.1	3.2	40.7	1.3
17-18				3.0	47.7	1.6	4.9	31.5	1.0	2.7	66.9	5.6	3.1	44.8	1.2	3.3	43.6	1.3
18-19	2.0	36.2	1.1	2.5	51.7	1.7	4.7	33.4	1.0	2.2	71.9	5.9	2.9	47.5	1.3	3.8	49.4	1.4
19-20				2.4	56.2	1.9	4.5	36.0	1.1	2.1	77.8	6.4	2.7	50.5	1.3	3.8	55.3	1.6
20-21	2.6	40.8	1.2	2.5	62.1	2.2	5.1	39.0	1.1	1.8	83.2	7.0	2.9	54.6	1.4	3.7	61.0	1.8
21-22				2.3	68.0	2.5	5.3	42.7	1.2	1.9	89.5	7.9	2.6	58.5	1.6	3.6	68.4	2.1
22-23	1.6	44.5	1.3	1.9	73.0	2.8	5.4	46.2	1.3	1.7	97.4	9.1	3.0	63.7	1.8	2.5	75.2	2.5
23-24				1.6	79.2	3.3	4.8	50.9	1.5	2.6	116.4	14.0	2.9	69.0	2.0	2.4	82.0	2.9
24-25	2.9	52.4	1.6	1.5	85.7	3.9	4.8	56.2	1.6	1.6	134.5	20.3	1.5	73.0	2.1	2.4	91.2	3.5
25-26				1.4	93.3	4.7	4.1	60.0	1.8	1.2	163.6	35.7	1.5	77.0	2.3	3.3	102.1	4.5
26-27	1.8	58.1	1.8	1.3	104.9	6.2	6.0	67.7	2.2	0.8			1.2	80.1	2.2	2.3	120.3	7.2
27-28				1.2	120.1	8.3	3.6	74.0	2.5	2.5			2.5	91.1	2.6	1.4	140.2	12.1
28-29	1.7	64.2	2.2	1.3	149.8	17.7	2.5	79.7	2.8	4.1			4.1	111.2	4.1	1.6	222.1	98.7
29-30				0.6	186.6	40.7	2.4	87.7	3.3	3.3			3.3	147.8	10.9	0.1		
30-31	1.5	70.8	2.5	0.2			2.1	94.4	3.8	0.9			0.9	173.8	20.1			
31-32				1.8	102.4	4.5	1.8	102.4	4.5	0.5			0.5					
32-33	2.7	85.1	3.9	1.4	110.0	5.3	1.4	110.0	5.3									
33-34				1.5	120.9	6.8	1.5	120.9	6.8									
34-35	2.1	106.9	7.1	1.3	134.8	9.4	1.3	134.8	9.4									
35-36				1.4	157.4	16.6	1.4	157.4	16.6									
36-37	1.5	152.3	27.5	1.0	218.0	75.8	1.0	218.0	75.8									
37-38				0.2			0.2											
38-39																		
39-40	0.6																	

^aCore SH3-1 was sectioned in 1 cm intervals until a depth of 10 cm; intervals below that depth are 2 cm.

The mean $\delta^{13}\text{C}$ was -26.4 ± 0.9 ‰ (Table 1). Variability was highest in the three upper intervals where the standard deviations were 2.5, 1.7, and 1.7 compared to a mean standard deviation of 0.6 ± 0.2 for the 3–30 cm depth intervals. The mean $\delta^{15}\text{N}$ was 3.1 ± 0.5 ‰ (Table 1). Standard deviations were relatively similar throughout all depths (0.4 ± 0.2 ‰). However, core SH3-1 had substantial variability with five intervals interspersed throughout the core that had $\delta^{15}\text{N}$ values greater than 4.0 ‰ (Figure 2).

3.2. Pb-210 Activities and CRS-Modeled Dates

The six cores show a net decrease in the activity of excess ^{210}Pb (Table 2). Each also exhibits lower activities in the near-surface intervals that correspond to dilution from Hurricane Wilma's input of marine carbonate sediment that is low in ^{210}Pb [Smoak *et al.*, 2013]. There are several unusually high peaks in $^{210}\text{Pb}_{\text{ex}}$ below 20 cm depth. This is likely due to advective mixing from crab burrows. The CRS dating model is relatively insensitive to mixing [Appleby and Oldfield, 1992], and these individual peaks do not alter results substantially. Core SH3-8 is an example of this; the largest of these peaks in $^{210}\text{Pb}_{\text{ex}}$ activities occurs at 27–30 cm depth. If this peak is manually removed so that the points are linearly interpolated to activity levels between the points above and below the peak, the resulting changes to the measured rates are relatively minor. The total age of the profile increases by ~ 20 years; most of the date changes occur in the bottommost $^{210}\text{Pb}_{\text{ex}}$ intervals where the ages are greater than 100 years. The 100 year rates remain largely the same, with accretion decreasing by 0.1 mm yr^{-1} and OC burial decreasing by $7 \text{ g m}^{-2} \text{ yr}^{-1}$.

3.3. Calculated Rates

Although there are numerous periods of increase or decrease between intervals in individual cores, in general, the rate profiles show a net decline with depth (Figures 3 and 4). As a result the integrated rates over 10, 50, and 100 years decrease in each core record. The 10 year average accumulation rate for IM is 1028 ± 568 , decreasing to $301 \pm 104 \text{ g m}^{-2} \text{ yr}^{-1}$ for the 100 year average (Table 3). There is a prominent peak of IM accumulation in the top three intervals of SH3-1 that requires a scale adjustment compared to that used for the other five cores. The 10 year average accumulation rate for OM is 462 ± 97 decreasing to $267 \pm 46 \text{ g m}^{-2} \text{ yr}^{-1}$ for the 100 year average (Table 3).

The 10 year average OC burial rate is 225 ± 61 , and decreases to $123 \pm 19 \text{ g m}^{-2} \text{ yr}^{-1}$ over the 100 year period. Variability for TN and TP accumulation rates shows the same general decline from the 10 year to 100 year averages, but both show extensive spatial variability at the 10 year level. The 10 year accumulation rate for TN is 13.8 ± 6.3 and $7.0 \pm 1.4 \text{ g m}^{-2} \text{ yr}^{-1}$ for the 100 year period. The 10 year accumulation rate for TP is 0.58 ± 0.25 and $0.20 \pm 0.08 \text{ g m}^{-2} \text{ yr}^{-1}$ for the 100 year period (Table 3).

The density-corrected accretion rate from all six cores is $4.8 \pm 1.0 \text{ mm yr}^{-1}$ at the 10 year period and $2.7 \pm 0.4 \text{ mm yr}^{-1}$ at the 100 year period (Table 3). Cores SH3-1 and SH3-5 show a marked increase in accretion in the near-surface intervals following hurricane Wilma, with rates that exceed 10 and 8 mm yr^{-1} , respectively (Figure 3). If the contributions from Hurricane Wilma in the period from 2000 to 2010 are excluded, the 100 yr mean accretion rate decreases only slightly to 2.6 ± 0.5 . Both rates match the tide gauge record of sea level rise ($2.24 \pm 0.16 \text{ mm yr}^{-1}$) from Key West, FL (approximately 120 km south of the research site), over the same time period [Maul and Martin, 1993; NOAA National Ocean Service, 2014].

4. Discussion

4.1. Temporal and Spatial Variability

The spatial variability between cores decreases substantially from short to long timescales as reflected in the decreasing mean rates and standard deviations with increasing age (Table 3; Figure 4). All of the rates measured here are highest during the most recent 10 year period, and decrease over the 50 and 100 year periods (Figure 5), thus supporting our first hypothesis. This has important implications for sampling strategies. This evidence of high spatial variability over short time spans supports the practice of using multiple observation stations for these types of measurements, similar to those using surface marker horizons [e.g., Cahoon and Lynch, 1997; Lovelock *et al.*, 2013; Saintilan *et al.*, 2013]. If longer-term measurements are made then the spatial variability is reduced and the likelihood of accounting for this is much higher with just 1–2 sampling locations. Additionally, this evidence indicates the importance of assigning a timescale of observation to any flux rates when making comparisons between sites. For example, even if each of the rates are reported in units of $\text{g m}^{-2} \text{ yr}^{-1}$, it is not appropriate to compare carbon

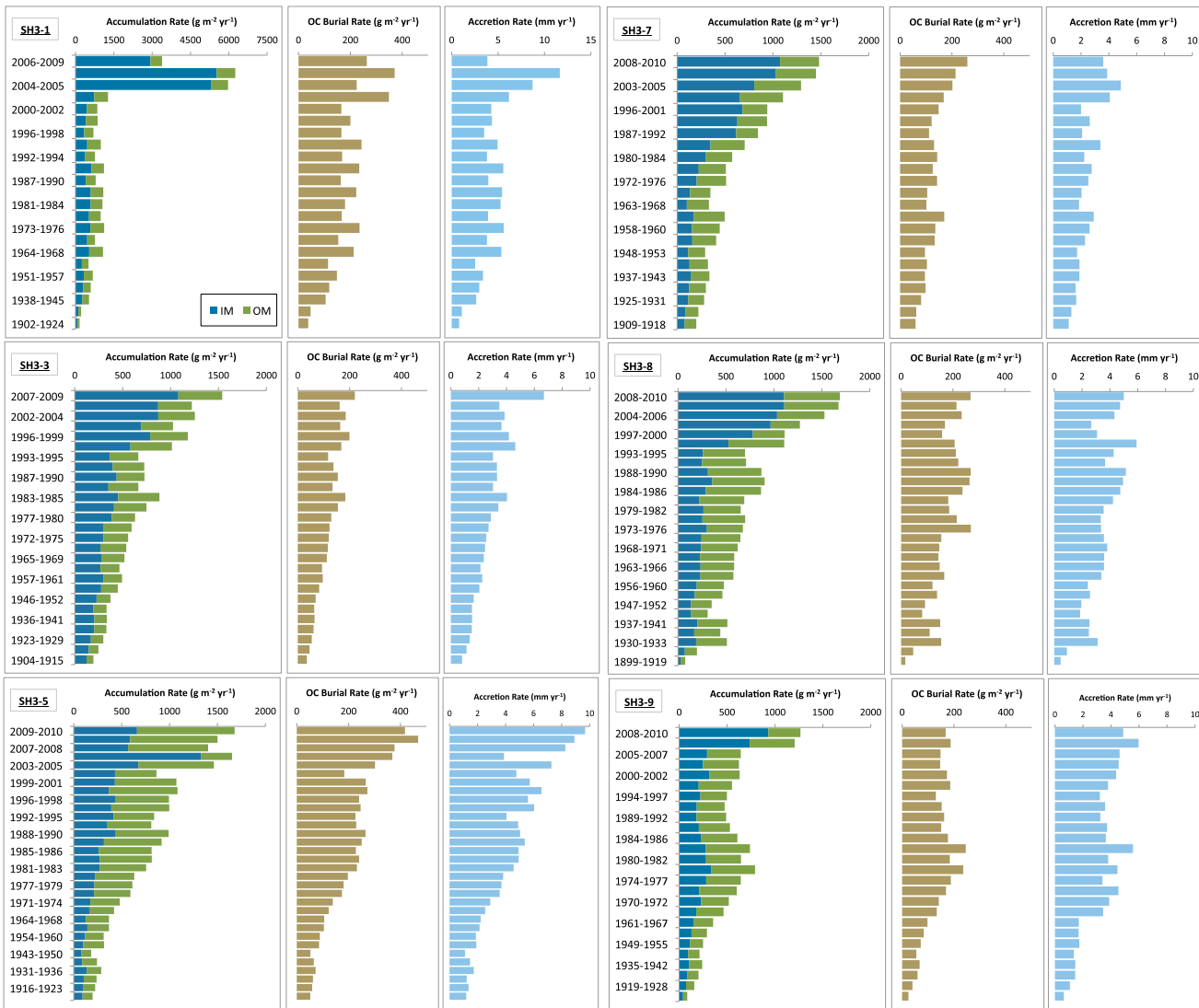


Figure 3. Profiles of inorganic and organic matter accumulation, OC burial, and accretion rates for each of the six soil cores. Note that the scales for SH3-1 IM and OM accumulation and accretion have been adjusted to account for the larger surface rates in that core [Smoak *et al.*, 2013].

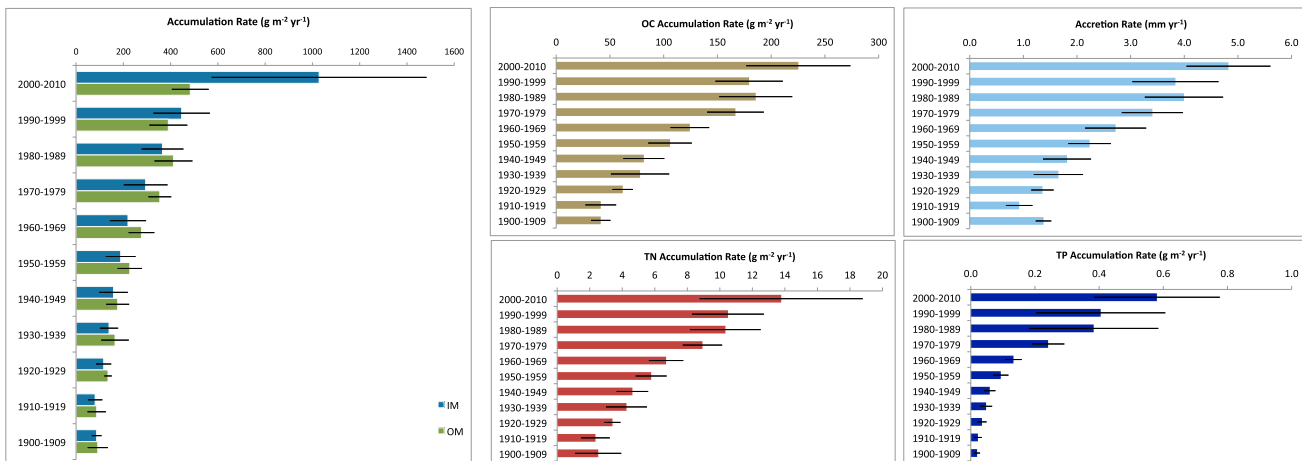


Figure 4. Site mean sediment accumulation rates aggregated by decade. Bars represent 95% confidence interval of the six core mean rates for each decade.

Table 3. Ten Year, 50 Year, and 100 Year Site Mean Rates

	Timescale	Site Mean	SD
Inorganic matter ($\text{g m}^{-2}\text{yr}^{-1}$)	10 year	1028	568
	50 year	471	177
	100 year	301	104
Organic matter ($\text{g m}^{-2}\text{yr}^{-1}$)	10 year	462	97
	50 year	380	73
	100 year	267	46
Organic carbon ($\text{g m}^{-2}\text{yr}^{-1}$)	10 year	225	61
	50 year	176	31
	100 year	123	19
Total nitrogen ($\text{g m}^{-2}\text{yr}^{-1}$)	10 year	13.8	6.3
	50 year	10.0	2.5
	100 year	7.0	1.4
Total phosphorous ($\text{g m}^{-2}\text{yr}^{-1}$)	10 year	0.58	0.25
	50 year	0.35	0.15
	100 year	0.20	0.08
Accretion (mm yr^{-1})	10 year	4.8	1.0
	50 year	3.7	0.7
	100 year	2.7	0.4

sequestration rates between sites when the measurements have been made using different dating techniques such as surface marker horizons (≤ 10 years), ^{137}Cs (~ 50 years), and ^{210}Pb (~ 100 years or greater [e.g., *Chmura et al., 2003; Mcleod et al., 2011; Breithaupt et al., 2012*]). Rather these rates should be reported as $\text{g m}^{-2}\text{yr}^{-1}$ per specified timescale when making these comparisons.

Because soil accretion and carbon sequestration in coastal wetlands are primarily of interest in the context of global sea level rise and climate change mitigation [*Grimsditch et al., 2012*], we find that the 50- to 100-year timeframes

provide the most conservative forecast of the regional long-term rates. Short-term measurements would likely overestimate the capacity for OC burial and accretion as surface sediments are most susceptible to processes such as erosion, remineralization, or pulse deposition events to name a few. However, there may be circumstances when the short-term rates are indicative of future trends. If a recent, long-lasting change has occurred in a sampling location (such as natural or anthropogenic alterations to wetland

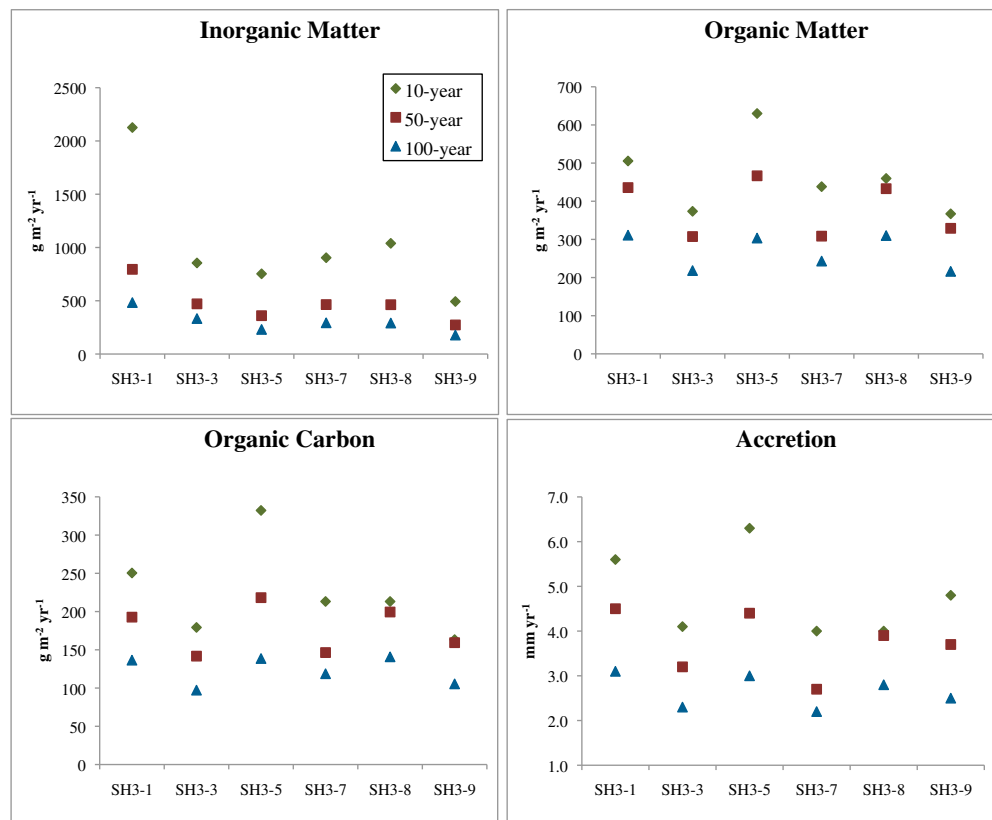


Figure 5. Ten year, 50 year, and 100 year integrated mean rates of inorganic matter accumulation, organic matter accumulation, organic carbon burial, and accretion for each of the six cores.

structure or hydrology), then it is conceivable that a short-term record that captures acceleration or deceleration in sedimentation rates as a response to a disturbance might provide the best indication of future trends. Examples include road construction [Harmon *et al.*, 2014], shrimp farm construction [Suárez-Abelenda *et al.*, 2014], abrupt tectonic change [Patel and Agoramoorthy, 2012] or direct impact of a large storm [Cahoon *et al.*, 2003]. But, unless such short-term changes can be categorically differentiated from the long-term steady-state cycles and processes of delivery and degradation, then observations from a longer period of record are more likely to provide a reliable prediction of future sediment accumulation rates.

These timescale specifications apply to both organic and inorganic sediments (Figure 5). The profiles show a change in the rate of OM and IM accumulation in each core during the past century suggesting that conditions of sedimentation and/or preservation have not been in steady state over the dated period [Burdige, 2006; Berner, 1972]. It should be noted that the amount of material present at the time of collection represents net sedimentation and preservation/degradation. Therefore, while there is an increase in the measured rates over the past century (Figure 4), there are multiple scenarios that can explain this outcome. An increase or decrease between any two intervals is driven by changes to the sediment delivery rate and/or to the sediment degradation or removal rate [Zimmerman and Canuel, 2000]. In other words, the profiles in Figure 4 can conceivably represent (a) a recent increase in delivery, (b) a recent increase in preservation, (c) the regular occurrence of ongoing degradation at each depth over the past century, or (d) some combination of the above including a recent increase combined with ongoing degradation. Further work is required to isolate the influence of individual mechanisms at work in this setting; however, we note the importance of their intermingling effects over the timescales in which we are interested.

One mechanism that has been well identified is the influence of Hurricane Wilma. That event is one line of evidence for increased delivery as a driver of high rates in the near-surface intervals. While the magnitude of the increase relative to previous intervals is most pronounced in core SH3-1 (Figure 3), each of the cores has its generally highest rates in intervals that have occurred following the year 2000. The Wilma signature of inorganic (largely carbonate) sediment is not uniform throughout these cores spatially nor is it uniform temporally. The inorganic accumulation rates in two cores have decreased following 2005 (Figure 3: SH3-1, SH3-5) while the others have remained at the same level or even increased since 2005. The OM accumulation rate in each of the cores is highest in these uppermost intervals; however, in cores 3, 7, 8, and 9 the increase is only slight. It is conceivable that these uppermost layers simply have higher OM mass in them because of the temporal proximity to a fresh, labile litter supply that over time will degrade and eventually become more like the rates present in the middle to lower depths of these cores. However, in cores SH3-1 and especially SH3-5, the near-surface rates of organic matter accumulation are substantially elevated above the underlying intervals. There are several possibilities for the elevated OM in these intervals including poststorm production [Whelan *et al.*, 2009] either caused by storm sediment provision of P [Castañeda-Moya *et al.*, 2010], normal poststorm recovery production, storm surge deposition of previously buried OM [Smoak *et al.*, 2013] or some combination of all of these.

The nutrient and stable isotope characterization of the soil similarly reflects a difference between the short- and long-term records. The average $\delta^{13}\text{C}$ values for all dated soil intervals are -26.4 ± 0.9 ‰ (Table 1). The highest variability is found in the top three intervals (Figure 2 and Table 3), indicating the presence of both autochthonous and allochthonous OM and the influence of hurricane Wilma's storm surge deposition. The surface intervals for all cores except SH3-5 and 9 show a strong positive excursion in $\delta^{13}\text{C}$ values of -25 to -22 (Figure 2). Enriched values like these suggest a nonmangrove source as evidenced by assessment of global mangrove litter averaging -28 to -30 ‰ [Kristensen *et al.*, 2008] and Shark River mangrove leaves and wood ranging from -27 to -31 ‰ [Fry and Smith, 2002; Mancera-Pineda *et al.*, 2009].

Additionally, core SH3-1 has the highest means and standard deviations of TN, $\delta^{15}\text{N}$, C:N, and N:P, indicative of its close proximity to the river's edge and the supply of allochthonous marine and algal sources of organic [Smoak *et al.*, 2013] and inorganic material, including Ca-bound P [Castañeda-Moya *et al.*, 2010]. The importance of Wilma on the soil characteristics of this site are reflected in the high flux rates of TN and TP in the last 10–50 years (Table 3). While the TP burial rates are somewhat lower than the global median, TN burial rates over the last five decades (especially for core SH3-1) exceed global median rates of $8.5 \text{ g m}^{-2} \text{ yr}^{-1}$ for mangrove wetlands (Table 4). The input of nutrients to the soil contributes to high forest productivity [Castañeda-Moya *et al.*, 2010] but potentially also leads to increased soil microbial respiration [Deegan *et al.*,

Table 4. Literature Values for TN and TP Soil Fluxes (aka Burial Rates)^a

Sampling Site	TN (g m ⁻² yr ⁻¹)	TP (g m ⁻² yr ⁻¹)	Source ^b
Shark River, FL	8.8	0.23	1
Shark River, FL	6.6	0.2	1
Shark River, FL	8.6	0.3	1
Shark River, FL	5.7	0.12	1
Shark River, FL	7.0		1
Shark River, FL	5.4	0.1	1
Sawi Bay, Thailand	8.3		2
Sawi Bay, Thailand	6.8		2
Sawi Bay, Thailand	11.0		2
Sawi Bay, Thailand	7.0		2
Perak, Malaysia	26.2		3
Perak, Malaysia	12.1		3
Perak, Malaysia	14.9		3
Perak, Malaysia	14.4		3
Perak, Malaysia	14.4		3
Perak, Malaysia	9.4		3
Jiulongjiang Estuary, China	49.0	31.4	4
Jiulongjiang Estuary, China	10.1	4.3	4
Jiulongjiang Estuary, China	12.8	5.5	4
Jiulongjiang Estuary, China	15.0	11.2	4
Jiulongjiang Estuary, China	16.3	12.2	4
Jiulongjiang Estuary, China	75.0	48.1	4
Irian Jaya, Indonesia	28.6		5
Irian Jaya, Indonesia	14.3		5
Irian Jaya, Indonesia	17.1		5
Irian Jaya, Indonesia	8.5		5
Yucatan Peninsula, Mexico ^c	3.9		6
Yucatan Peninsula, Mexico ^c	4.0		6
Yucatan Peninsula, Mexico ^c	4.0		6
Yucatan Peninsula, Mexico ^c	3.7		6
Yucatan Peninsula, Mexico ^c	4.9		6
Terminos Lagoon, Mexico	5.8	0.8	7
Terminos Lagoon, Mexico	1.6	0.7	7
Terminos Lagoon, Mexico	3.9	0.7	7
Terminos Lagoon, Mexico	4.8	0.5	7
Terminos Lagoon, Mexico	2.7	0.1	7
Rookery Bay, Florida	5.3	0.2	7
Rookery Bay, Florida	4.2	0.2	7
Rookery Bay, Florida	4.7	0.2	7
Rookery Bay, Florida	6.0	0.2	7
Ilha Grande, Brazil	3.1		8
Tamandare, Brazil	15.9		9
Tamandare, Brazil	7.2		9
Cananeia, Brazil	12.2	1.7	10
Cananeia, Brazil	16.1	2.6	10
Cubatão, Brazil	33.2	13.8	11
Cubatão, Brazil	28.5	20.6	11

^aThe mean and median TN rates are 12.5 and 8.9 g m⁻² yr⁻¹, respectively. The mean and median TP rates are 6.5 and 0.7 g m⁻² yr⁻¹, respectively. If values from anthropogenically disturbed locations (Jiulongjiang, China and Cubatão, Brazil) are excluded, then the respective mean rates for TN and TP are 8.9 and 0.5 g m⁻² yr⁻¹.

^b1 = This study; 2 = Alongi et al. [2002]; 3 = Alongi et al. [2004]; 4 = Alongi et al. [2005]; 5 = Brunskill et al. [2004]; 6 = Gonnee et al. [2004]; 7 = Lynch [1989]; 8 = Sanders et al. [2010a]; 9 = Sanders et al. [2010b]; 10 = Sanders et al. [2012]; and 11 = Sanders et al. [2014].

^cValues from figures were estimated using Get Data Graph Digitizer (<http://getdata-graph-digitizer.com/>).

2012; Kirwan and Megonigal, 2013; Krauss et al., 2014] as well as a more diverse source of OM in the surface soil including labile microalgae and detritus with low carbon burial efficiencies [Sanders et al., 2014].

4.2. Carbon Burial

The 100 year mean OC burial rate for this site is 123 ± 19 g m⁻² yr⁻¹ (Table 3), which equates to 10.5% of Net Ecosystem Production [Barr et al., 2010]. This mean rate is relatively low compared to the global geometric mean of 163 (+40; -31) g OC m⁻² yr⁻¹ [Breithaupt et al., 2012] and is not greatly different from rates of OC burial at other mangrove sites in Florida, thus rejecting our second hypothesis that carbon burial is a function of high primary production and peat soil with a high percentage of OC. At a site approximately 7 km north of this location in the Everglades, Smoak et al. [2013] measured a centennial rate of 168 g OC m⁻² yr⁻¹ in a single core, a rate slightly higher than any single core at this site over the same time period. Smoak et al. [2013] proposed that a portion of the OC from that site could be attributed to the substantially higher deposition of organic material during Hurricane Wilma at the Harney River site compared to the Shark River site. In Rookery Bay, FL, 96 km northwest of this location, Lynch [1989] used ²¹⁰Pb-based geochronologies from four cores to measure a mean centennial OC burial rate of 86 ± 13 g m⁻² yr⁻¹. Our 50 year mean rate of 176 ± 31 is similar to the rate of 147 g OC m⁻² yr⁻¹ that was measured in the Florida Keys using the ¹³⁷Cs dating method based on a peak fallout signature in 1963 [Callaway et al., 1997].

It is somewhat surprising that this location within the Everglades has a low OC burial rate. Even though the aboveground characteristics

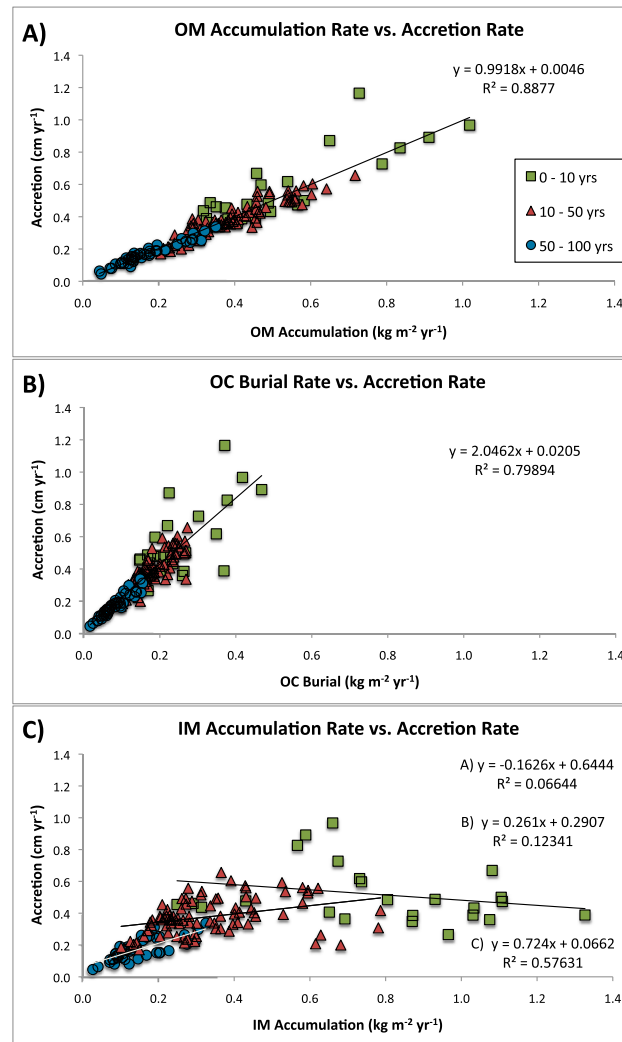


Figure 6. Relationship between (a) organic matter accumulation, (b) organic carbon burial, and (c) inorganic matter accumulation and accretion rates for all dated soil intervals (≤ 100 years) ($n = 161$ for OM and OC; $n = 158$ for IM because three outlier samples from Hurricane Wilma in core SH3-1 have been removed for this analysis). In Figure 6c, trend line equations and R^2 values are for the three interval age classes 0–10 years (equation A), 10–50 years (equation B), and 50–100 years (equation C). If the three age classes are analyzed together the linear regression trend line equation is: $y = 0.1584x + 0.2787$ and the R^2 is 0.33.

indicate a highly productive forest [Barr et al., 2010; Castañeda-Moya et al., 2013; Simard et al., 2006] and the peat soil has a high percentage of OC (Table 1) [Castañeda-Moya et al., 2011], these traits alone are insufficient to make a qualitative prediction of a site's OC burial rate (i.e., higher or lower than the global mean). Recently assessed OC burial rates in mangroves in Port Aransas, Texas provide a strong contrast based on these site characteristics. In Port Aransas rates of $270 \pm 12 \text{ g OC m}^{-2} \text{ yr}^{-1}$ were measured using ^{137}Cs and $253 \pm 11 \text{ g OC m}^{-2} \text{ yr}^{-1}$ based on the ^{210}Pb -derived 1963 date [Bianchi et al., 2013]. Our 50 year mean OC burial rate is 176 ± 31 (Table 3), substantially lower than the Texas rates. The mangroves in Texas are between 1 and 2 m tall whereas those at our site in the lower Everglades are between 13–19 m tall. Additionally, in Port Aransas the soil OC% for four cores range from 0.1 to 11.37% but the majority of the values are less than 6% [Bianchi et al., 2013]. At our Everglades site the mean OC% is 24 ± 6 (Table 1). The OC burial rates from these two sites disprove a notion raised in the literature that soil OC% and the rate of OC burial are positively correlated [Kristensen et al., 2008; Breithaupt et al., 2012]. More research is needed to specifically examine the relationship of soil OC density (as opposed to OC%) and productivity to OC burial rates, but the limited data mentioned here demonstrate that other factors exert a significant control. In addition to the potential increase in soil respiration from elevated nutrient concentrations mentioned earlier, these other factors likely include belowground productivity and its ratio to aboveground

productivity [Castañeda-Moya et al., 2013; Lovelock, 2008], root density/turnover times [Adame et al., 2014; Castañeda-Moya et al., 2011], the rate of particulate and dissolved organic and inorganic carbon export [Bergamaschi et al., 2012; Maher et al., 2013; Sanders et al., 2010b], the extent of burrowing and bioturbation [Smith et al., 1991; Andretta et al., 2013], and the supply of inorganic sediments which may aid in sealing organic matter off from remineralization.

4.3. Accretion

The accumulation rates of OM, IM, and OC each influence accretion rates somewhat differently (Figure 6). There is a substantial amount of spatial and temporal variability in IM accumulation, and thus, the data have been subjected to three separate age-related regressions with accretion. Note that these regressions are for the measured rates of each individual soil interval in the specified age ranges; they are not the depth-

integrated averages (i.e., Figure 5). While there is nearly a 1:1 relationship between OM accumulation and accretion, the slopes and R^2 values for IM over the 0–10 and 10–50 year intervals are much shallower. Inorganic matter has a much lower and less predictable influence on site accretion over these timescales at this site in the Everglades. The density of OM is lower than that of IM, and as a result OM can contribute to a higher accretion rate. The y intercept for OM is approximately 0; however, for IM the y intercept for all three age classes is 0.6 to 6.4 mm yr⁻¹. This range indicates the average magnitude of the accretion contribution made by OM relative to IM. While the evidence here indicates that IM accumulation has only a minor direct influence on sediment accretion, this does not preclude a substantial indirect influence that may occur because of P-fertilization in the storm surge deposition [Castañeda-Moya *et al.*, 2010] and a subsequent increase in organic matter production. The IM accumulation is relatively well correlated with accretion for the intervals between the ages of 50–100 years, although the slope is about 25% shallower than that for OM. The difference in slopes may be attributed to greater compaction and consolidation for these depths, or it might indicate an increase in the supply of marine carbonate sediments from storm surge in recent years.

Mangrove soil OC is most often discussed in the context of greenhouse gas sequestration, but here it also serves as a soil-building component of vital importance to the ecosystem. If OC burial rates are regressed with accretion rates the R^2 is 0.80 and the slope is 2.05 (Figure 6), reflecting the importance that OC provides to the soil structure here. Without the 25% of soil mass that is OC (Table 1), the forest floor of this site would be considerably lower than its present position and would consequently endure greater physical stress in addition to altered redox conditions from substantially increased periods and extents of inundation [Gilman *et al.*, 2007; Lu *et al.*, 2013]. As previous research has noted, the autochthonous production of organic material is of considerable importance to mangroves growing in locations with little to no terrigenous sediment supply [McKee, 2011; McKee *et al.*, 2007; Parkinson *et al.*, 1994; Woodroffe, 1990]. As it is, this OM and OC does not contribute uniformly to surface accretion but is able to shrink and swell in response to various hydrologic conditions at different depths of the soil column [Whelan *et al.*, 2005].

Although these findings indicate that this location in the Everglades is keeping pace with sea level rise, research of this nature is needed on a much wider spatial scale to assess the net soil accumulation rates across the greater coastal Everglades. As has been shown in estuaries in China and Malaysia, single site assessments of accretion and accumulation may not accurately account for cumulative losses occurring elsewhere in the system [Alongi, 2011]. As was similarly noted by Smoak *et al.* [2013], one of the significant implications may be that the addition of material at this site occurs at the expense of other locations on the seaward edges of the Everglades.

5. Conclusions

The importance of OC in mangrove wetlands may be quantified in terms of the rate at which CO₂ is sequestered as well as the rate at which it contributes to soil building. The latter function is especially important in carbonate platform environments that have minimal terrigenous sediment inputs. Our findings indicate that the coastal Everglades, with highly productive mangroves and high soil OC content bury OC relatively slowly. The importance of hurricane events on the soil characteristics of this site are reflected in the high flux rates of TN and TP in the most recent 10–50 years. The storm surge-derived marine material increases aboveground primary production but may increase soil remineralization, contributing to the relatively slow rate of OC burial. The combination of high productivity with relatively low OC burial raises important questions for future research such as how well the rates at this site represent the coastal Everglades, and how autochthonous and allochthonous rates of production relate to OC burial. A second important finding is the need to consider changing rates over time, and thus changes to the dominant processes occurring during sedimentation and within the soil column. Results here suggest that short-term measurements are unsuitable for assessing longer-term trends. Additionally, because carbon sequestration is primarily of interest in the context of global climate change mitigation, the 100 year timeframe is of central importance. Short-term C-sequestration measurements should be taken with caution because these rates may represent only partial cycles rather than long-term trends, and overestimation of long-term sequestration rates is likely.

Acknowledgments

Core data not supplied in primary tables for this paper are available in Table S1 in the supporting information. This material is based upon work supported by the National Science Foundation under South Florida Water, Sustainability & Climate grant 1204079 to J.M. Smoak. J.L. Breithaupt is grateful for funding support through the University of South Florida College of Marine Science fellowships provided by Anne and Werner Von Rosenstiel and the St. Petersburg Downtown Partnership, as well as a travel grant provided by the Florida Coastal Everglades Long-term Ecological Research program (supported by the National Science Foundation under grant DBI-0620409). T.J. Smith III was funded by the Environments Program of the Ecosystems Mission Area and the Greater Everglades Priority Ecosystems Studies Program of the U.S. Geological Survey. J.M. Smoak received funding from National Science Foundation and U.S. Geological Survey, Southeast Ecological Science Center. C.J. Sanders is supported by a Southern Cross University postdoctoral fellowship. The authors thank Tom Harmon, Luciana Sanders, Gordon Anderson, Karen Balentine, Ginger Tiling-Range, and Paul Nelson for their assistance with field sampling and laboratory processing. Any use of trade, product, or firm names is for descriptive purposes only and does not imply endorsement by the U.S. government.

References

- Adame, M. F., J. B. Kauffman, I. Medina, J. N. Gamboa, O. Torres, J. P. Caamal, M. Reza, and J. A. Herrera-Silveira (2013), Carbon stocks of tropical coastal wetlands within the karstic landscape of the Mexican Caribbean, *PLoS One*, *8*, e56569, doi:10.1371/journal.pone.0056569.
- Adame, M. F., C. Teutli, N. S. Santini, J. P. Caamal, A. Zaldívar-Jiménez, R. Hernández, and J. A. Herrera-Silveira (2014), Root biomass and production of mangroves surrounding a karstic oligotrophic coastal lagoon, *Wetlands*, doi:10.1007/s13157-014-0514-5.
- Alongi, D. M. (2011), Carbon payments for mangrove conservation: Ecosystem constraints and uncertainties of sequestration potential, *Environ. Sci. Policy*, *14*, 462–470, doi:10.1016/j.envsci.2011.02.004.
- Alongi, D. M., G. Wattayakorn, J. Pfitzner, and F. Tirendi (2001), Organic carbon accumulation and metabolic pathways in sediments of mangrove forests in southern Thailand, *Mar. Geol.*, *179*, 85–103, doi:10.1016/S0025-3227(01)00195-5.
- Alongi, D. M., L. Trott, G. Wattayakorn, and B. F. Clough (2002), Below-ground nitrogen cycling in relation to net canopy production in mangrove forests of southern Thailand, *Mar. Biol.*, *140*, 855–864, doi:10.1007/s00227-001-0757-6.
- Alongi, D. M., A. Sasekumar, V. C. Chong, J. Pfitzner, L. A. Trott, F. Tirendi, P. Dixon, and G. J. Brunskill (2004), Sediment accumulation and organic material flux in a managed mangrove ecosystem: Estimates of land–ocean–atmosphere exchange in peninsular Malaysia, *Mar. Geol.*, *208*, 383–402, doi:10.1016/j.margeo.2004.04.016.
- Alongi, D. M., J. Pfitzner, L. A. Trott, F. Tirendi, P. Dixon, and D. W. Klumpp (2005), Rapid sediment accumulation and microbial mineralization in forests of the mangrove in the Jiulongjiang Estuary, China, *Estuarine Coastal Shelf Sci.*, *63*, 605–618, doi:10.1016/j.ecss.2005.01.004.
- Alongi, D. M., L. A. Trott, F. Tirendi, A. D. McKinnon, and M. C. Undu (2008), Growth and development of mangrove forests overlying smothered coral reefs, Sulawesi and Sumatra, Indonesia, *Mar. Ecol. Prog. Ser.*, *375*, 97–109, doi:10.3354/meps07661.
- Andreetta, A., M. Fusi, I. Cameldi, F. Cimò, S. Carnicelli, and S. Cannicci (2013), Mangrove carbon sink. Do burrowing crabs contribute to sediment carbon storage? Evidence from a Kenyan mangrove system, *J. Sea Res.*, *85*, 524–533, doi:10.1016/j.seares.2013.08.010.
- Appleby, P. G., and F. Oldfield (1978), The calculation of Lead-210 dates assuming a constant rate of supply of unsupported ²¹⁰Pb to the sediment, *Catena*, *5*, 1–8.
- Appleby, P. G., and F. Oldfield (1992), Application of ²¹⁰Pb to sedimentation studies, in *Uranium-Series Disequilibrium: Applications to Earth, Marine & Environmental Sciences*, edited by M. Ivanovich and R. S. Harmon, pp. 731–778, Oxford Univ. Press, Oxford, U. K.
- Appleby, P. G., P. J. Nolan, F. Oldfield, N. Richardson, and S. R. Higgitt (1988), ²¹⁰Pb dating of lake sediments and ombrotrophic peats by gamma assay, *Sci. Total Environ.*, *69*, 157–177.
- Barr, J. G., V. Engel, J. D. Fuentes, J. C. Ziemann, T. L. O'Halloran, T. J. Smith, and G. H. Anderson (2010), Controls on mangrove forest-atmosphere carbon dioxide exchanges in western Everglades National Park, *J. Geophys. Res.*, *115*, G02020, doi:10.1029/2009JG001186.
- Barr, J. G., V. Engel, T. J. Smith, and J. D. Fuentes (2011), Hurricane disturbance and recovery of energy balance, CO₂ fluxes and canopy structure in a mangrove forest of the Florida Everglades, *Agric. For. Meteorol.*, doi:10.1016/j.agrformet.2011.07.022.
- Bergamaschi, B. A., D. P. Krabbenhoft, G. R. Aiken, E. Patino, D. G. Rumbold, and W. H. Orem (2012), Tidally driven export of dissolved organic carbon, total mercury, and methylmercury from a mangrove-dominated estuary, *Environ. Sci. Technol.*, *46*, 1371–1378, doi:10.1021/es2029137.
- Berner, R. A. (1972), Chemical kinetic models of early diagenesis, *J. Geol. Educ.*, *20*, 267–272.
- Bianchi, T. S., M. A. Allison, J. Zhao, X. Li, R. S. Comeaux, R. A. Feagin, and R. W. Kulawardhana (2013), Historical reconstruction of mangrove expansion in the Gulf of Mexico: Linking climate change with carbon sequestration in coastal wetlands, *Estuarine Coastal Shelf Sci.*, *119*, 7–16, doi:10.1016/j.ecss.2012.12.007.
- Bouillon, S., et al. (2008), Mangrove production and carbon sinks: A revision of global budget estimates, *Global Biogeochem. Cycles*, *22*, GB2013, doi:10.1029/2007GB003052.
- Breithaupt, J. L., J. M. Smoak, T. J. Smith, C. J. Sanders, and A. Hoare (2012), Organic carbon burial rates in mangrove sediments: Strengthening the global budget, *Global Biogeochem. Cycles*, *26*, GB3011, doi:10.1029/2012GB004375.
- Brunskill, G., I. Zagorskis, J. Pfitzner, and J. Ellison (2004), Sediment and trace element depositional history from the Ajkwa River estuarine mangroves of Irian Jaya (West Papua), Indonesia, *Cont. Shelf Res.*, *24*, 2535–2551, doi:10.1016/j.csr.2004.07.024.
- Bui, T. H. H., and S. Y. Lee (2014), Does “you are what you eat” apply to mangrove grapsid crabs?, *PLoS One* *9*, e89074, doi:10.1371/journal.pone.0089074.
- Burdige, D. J. (2006), *Geochemistry of Marine Sediments*, Princeton Univ. Press, Princeton, N. J.
- Cahoon, D. R., and J. C. Lynch (1997), Vertical accretion and shallow subsidence in a mangrove forest of southwestern Florida, U.S.A., *Mangroves Salt Marshes*, *1*(3), 173–186.
- Cahoon, D., P. Hensel, and J. Rybczyk (2003), Mass tree mortality leads to mangrove peat collapse at Bay Islands, Honduras after Hurricane Mitch, *J. Ecol.*, *91*, 1093–1105.
- Callaway, J., R. DeLaune, and W. Patrick Jr. (1997), Sediment accretion rates from four coastal wetlands along the Gulf of Mexico, *J. Coastal Res.*, *13*, 181–191.
- Castañeda-Moya, E., R. R. Twilley, V. H. Rivera-Monroy, K. Zhang, S. E. Davis, and M. Ross (2010), Sediment and nutrient deposition associated with Hurricane Wilma in mangroves of the Florida Coastal Everglades, *Estuaries Coasts*, *33*, 45–58, doi:10.1007/s12237-009-9242-0.
- Castañeda-Moya, E., R. R. Twilley, V. H. Rivera-Monroy, B. D. Marx, C. Coronado-Molina, and S. M. L. Ewe (2011), Patterns of root dynamics in mangrove forests along environmental gradients in the Florida Coastal Everglades, USA, *Ecosystems*, *14*, 1178–1195, doi:10.1007/s10021-011-9473-3.
- Castañeda-Moya, E., R. R. Twilley, and V. H. Rivera-Monroy (2013), Allocation of biomass and net primary productivity of mangrove forests along environmental gradients in the Florida Coastal Everglades, USA, *For. Ecol. Manage.*, *307*, 226–241, doi:10.1016/j.foreco.2013.07.011.
- Chen, R., and R. Twilley (1999a), A simulation model of organic matter and nutrient accumulation in mangrove wetland soils, *Biogeochemistry*, *44*, 93–118, doi:10.1007/BF00993000.
- Chen, R., and R. Twilley (1999b), Patterns of mangrove forest structure and soil nutrient dynamics along the Shark River estuary, Florida, *Estuaries Coasts*, *22*, 955–970.
- Childers, D., J. Boyer, S. Davis, and C. Madden (2006), Relating precipitation and water management to nutrient concentrations in the oligotrophic “upside-down” estuaries of the Florida Everglades, *Limnol. Oceanogr.*, *51*, 602–616.
- Chmura, G. L., S. C. Anisfeld, D. R. Cahoon, and J. C. Lynch (2003), Global carbon sequestration in tidal, saline wetland soils, *Global Biogeochem. Cycles*, *17*(4), 1111, doi:10.1029/2002GB001917.
- Costanza, R., O. Pérez-Maqueo, M. L. Martinez, P. Sutton, S. J. Anderson, and K. Mulder (2008), The value of coastal wetlands for hurricane protection, *Ambio*, *37*, 241–248.
- Deegan, L. A., D. S. Johnson, R. S. Warren, B. J. Peterson, J. W. Fleeger, S. Fagherazzi, and W. M. Wollheim (2012), Coastal eutrophication as a driver of salt marsh loss, *Nature*, *490*(7420), 388–392.

- Dittmar, T., N. Hertkorn, G. Kattner, and R. J. Lara (2006), Mangroves, a major source of dissolved organic carbon to the oceans, *Global Biogeochem. Cycles*, *20*, GB1012, doi:10.1029/2005GB002570.
- Donato, D. C., J. B. Kauffman, D. Murdiyasar, S. Kurnianto, M. Stidham, and M. Kanninen (2011), Mangroves among the most carbon-rich forests in the tropics, *Nat. Geosci.*, *4*, 293–297, doi:10.1038/ngeo1123.
- Donato, D. C., J. B. Kauffman, R. A. Mackenzie, A. Ainsworth, and A. Z. Pfeleger (2012), Whole-island carbon stocks in the tropical Pacific: Implications for mangrove conservation and upland restoration, *J. Environ. Manage.*, *97*, 89–96, doi:10.1016/j.jenvman.2011.12.004.
- Duarte, C. M., J. J. Middelburg, and N. Caraco (2005), Major role of marine vegetation on the oceanic carbon cycle, *Biogeosciences*, *2*, 1–8, doi:10.5194/bg-2-1-2005.
- Fourqurean, J. W., J. C. Zieman, and G. V. N. Powell (1992), Phosphorus limitation of primary production in Florida Bay: Evidence from C:N:P ratios of the dominant seagrass *Thalassia testudinum*, *Limnol. Oceanogr.*, *37*, 162–171, doi:10.4319/lo.1992.37.1.0162.
- Fry, B., and T. Smith (2002), Stable isotope studies of red mangroves and filter feeders from the Shark River estuary, Florida, *Bull. Mar. Sci.*, *70*, 871–890.
- Gilman, E., J. Ellison, and R. Coleman (2007), Assessment of mangrove response to projected relative sea-level rise and recent historical reconstruction of shoreline position, *Environ. Monit. Assess.*, *124*, 105–30, doi:10.1007/s10661-006-9212-y.
- Giri, C., E. Ochieng, L. L. Tieszen, Z. Zhu, A. Singh, T. Loveland, J. Masek, and N. Duke (2011), Status and distribution of mangrove forests of the world using earth observation satellite data, *Global Ecol. Biogeogr.*, *20*, 154–159, doi:10.1111/j.1466-8238.2010.00584.x.
- Gonneea, M. E., A. Paytan, and J. A. Herrera-Silveira (2004), Tracing organic matter sources and carbon burial in mangrove sediments over the past 160 years, *Estuarine Coastal Shelf Sci.*, *61*, 211–227, doi:10.1016/j.ecss.2004.04.015.
- Grimsditch, G., J. Alder, T. Nakamura, R. Kenchington, and J. Tamelander (2012), The blue carbon special edition—Introduction and overview, *Ocean Coastal Manage.*, *1*, 1–4, doi:10.1016/j.ocecoaman.2012.04.020.
- Harmon, T. S., J. M. Smoak, M. N. Waters, and C. J. Sanders (2014), Hydrologic fragmentation-induced eutrophication in Dove Sound, Upper Florida Keys, USA, *Environ. Earth Sci.*, *71*, 4387–4395, doi:10.1007/s12665-013-2832-y.
- Jennerjahn, T., and V. Ittekkot (2002), Relevance of mangroves for the production and deposition of organic matter along tropical continental margins, *Naturwissenschaften*, *89*, 23–30, doi:10.1007/s00114-001-0283-x.
- Kauffman, J. B., C. Heider, T. G. Cole, K. A. Dwire, and D. C. Donato (2011), Ecosystem carbon stocks of Micronesian mangrove forests, *Wetlands*, *31*, 343–352, doi:10.1007/s13157-011-0148-9.
- Kirwan, M. L., and J. P. Megonigal (2013), Tidal wetland stability in the face of human impacts and sea-level rise, *Nature*, *504*, 53–60, doi:10.1038/nature12856.
- Krauss, K. W., T. W. Doyle, R. R. Twilley, V. H. Rivera-Monroy, and J. K. Sullivan (2006), Evaluating the relative contributions of hydroperiod and soil fertility on growth of south Florida mangroves, *Hydrobiologia*, *569*, 311–324, doi:10.1007/s10750-006-0139-7.
- Krauss, K. W., K. L. McKee, C. E. Lovelock, D. R. Cahoon, N. Saintilan, R. Reef, and L. Chen (2014), How mangrove forests adjust to rising sea level, *New Phytol.*, *202*, 19–34, doi:10.1111/nph.12605.
- Kristensen, E., S. Bouillon, T. Dittmar, and C. Marchand (2008), Organic carbon dynamics in mangrove ecosystems: A review, *Aquat. Bot.*, *89*, 201–219, doi:10.1016/j.aquabot.2007.12.005.
- Lovelock, C. E. (2008), Soil respiration and belowground carbon allocation in mangrove forests, *Ecosystems*, *11*, 342–354, doi:10.1007/s10021-008-9125-4.
- Lovelock, C. E., M. F. Adame, V. Bennion, M. Hayes, J. O'Mara, R. Reef, and N. S. Santini (2013), Contemporary rates of carbon sequestration through vertical accretion of sediments in mangrove forests and saltmarshes of South East Queensland Australia, *Estuaries and Coasts*, doi:10.1007/s12237-013-9702-4.
- Lu, W., L. Chen, W. Wang, N. Fung-Yee Tam, and G. Lin (2013), Effects of sea level rise on mangrove *Avicennia* population growth, colonization and establishment: Evidence from a field survey and greenhouse manipulation experiment, *Acta Oecol.*, *49*, 83–91, doi:10.1016/j.actao.2013.03.009.
- Lynch, J. C. (1989), *Sedimentation and Nutrient Accumulation in Mangrove Ecosystems of the Gulf of Mexico*, Univ. of Southwestern La., Lafayette.
- Lynch, J. C., J. R. Meriwether, B. A. McKee, F. Vera-Herrera, and R. R. Twilley (1989), Recent accretion in mangrove ecosystems based on ¹³⁷Cs and ²¹⁰Pb, *Estuaries*, *12*, 284–299.
- Maher, D. T., I. R. Santos, J. Gleeson, and B. D. Eyre (2013), Groundwater-derived dissolved inorganic and organic carbon exports from a mangrove tidal creek: The missing mangrove carbon sink?, *Limnol. Oceanogr.*, *58*, 475–488, doi:10.4319/lo.2013.58.2.0475.
- Mancera-Pineda, J. E., R. R. Twilley, and V. H. Rivera-Monroy (2009), Carbon ($\delta^{13}\text{C}$) and Nitrogen ($\delta^{15}\text{N}$) isotopic discrimination in mangroves in Florida coastal Everglades as a function of environmental stress, *Contrib. Mar. Sci.*, *38*, 109–129.
- Maul, G., and D. Martin (1993), Sea level rise at Key West, Florida, 1846–1992: America's longest instrument record?, *Geophys. Res. Lett.*, *20*, 1955–1958, doi:10.1029/93GL02371.
- McKee, K. L. (2011), Biophysical controls on accretion and elevation change in Caribbean mangrove ecosystems, *Estuarine Coastal Shelf Sci.*, *91*, 475–483, doi:10.1016/j.ecss.2010.05.001.
- McKee, K. L., D. R. Cahoon, and I. C. Feller (2007), Caribbean mangroves adjust to rising sea level through biotic controls on change in soil elevation, *Global Ecol. Biogeogr.*, *16*, 545–556, doi:10.1111/j.1466-8238.2007.00317.x.
- Mcleod, E., G. L. Chmura, S. Bouillon, R. Salm, M. Björk, C. M. Duarte, C. E. Lovelock, W. H. Schlesinger, and B. R. Silliman (2011), A blueprint for blue carbon: Toward an improved understanding of the role of vegetated coastal habitats in sequestering CO₂, *Front. Ecol. Environ.*, *9*, 552–560, doi:10.1890/110004.
- Nagelkerken, I., et al. (2008), The habitat function of mangroves for terrestrial and marine fauna: A review, *Aquat. Bot.*, *89*, 155–185, doi:10.1016/j.aquabot.2007.12.007.
- NOAA National Ocean Service (2014), Mean sea level trend key West Florida. [Available at http://tidesandcurrents.noaa.gov/sltrends/sltrends_station.shtml?stnid=8724580.]
- Noe, G. B., D. L. Childers, and R. D. Jones (2001), Phosphorus biogeochemistry and the impact of phosphorus enrichment: Why is the Everglades so unique?, *Ecosystems*, *4*, 603–624, doi:10.1007/s10021-001-0032-1.
- Parkinson, R., R. DeLaune, and J. White (1994), Holocene sea-level rise and the fate of mangrove forests within the wider Caribbean region, *J. Coastal Res.*, *10*, 1077–1086.
- Patel, P., and G. Agoramorthy (2012), India's rare inland mangroves deserve protection, *Environ. Sci. Technol.*, *46*, 4261–4262, doi:10.1021/es301062v.
- Pendleton, L., et al. (2012), Estimating global “blue carbon” emissions from conversion and degradation of vegetated coastal ecosystems, *PLoS One*, *7*, e43542, doi:10.1371/journal.pone.0043542.
- Romigh, M. M., S. E. Davis, V. H. Rivera-Monroy, and R. R. Twilley (2006), Flux of organic carbon in a riverine mangrove wetland in the Florida Coastal Everglades, *Hydrobiologia*, *569*, 505–516, doi:10.1007/s10750-006-0152-x.

- Saintilan, N., K. Rogers, D. Mazumder, and C. Woodroffe (2013), Allochthonous and autochthonous contributions to carbon accumulation and carbon store in southeastern Australian coastal wetlands, *Estuarine Coastal Shelf Sci.*, *128*, 84–92, doi:10.1016/j.ecss.2013.05.010.
- Sanders, C. J., J. M. Smoak, A. S. Naidu, D. R. Araripe, L. M. Sanders, and S. R. Patchineelam (2010a), Mangrove forest sedimentation and its reference to sea level rise, Cananea, Brazil, *Environ. Earth Sci.*, *60*(6), 1291–1301, doi:10.1007/s12665-009-0269-0.
- Sanders, C. J., J. M. Smoak, A. S. Naidu, L. M. Sanders, and S. R. Patchineelam (2010b), Organic carbon burial in a mangrove forest, margin and intertidal mud flat, *Estuarine Coastal Shelf Sci.*, *90*(3), 168–172, doi:10.1016/j.ecss.2010.08.013.
- Sanders, C. J., J. M. Smoak, M. N. Waters, L. M. Sanders, N. Brandini, and S. R. Patchineelam (2012), Organic matter content and particle size modifications in mangrove sediments as responses to sea level rise, *Mar. Environ. Res.*, *77*, 150–155, doi:10.1016/j.marenvres.2012.02.004.
- Sanders, C., et al. (2014), Elevated rates of organic carbon, nitrogen and phosphorus accumulation in a highly impacted mangrove wetland, *Geophys. Res. Lett.*, *41*, 2475–2480, doi:10.1002/2014GL059789.
- Siikamäki, J., J. N. Sanchirico, and S. L. Jardine (2012), Global economic potential for reducing carbon dioxide emissions from mangrove loss, *Proc. Natl. Acad. Sci. U.S.A.*, *109*, 14,369–14,374, doi:10.1073/pnas.1200519109.
- Simard, M., K. Zhang, V. H. Rivera-Monroy, M. S. Ross, P. L. Ruiz, E. Castañeda-Moya, R. R. Twilley, and E. Rodriguez (2006), Mapping height and biomass of mangrove forests in Everglades National Park with SRTM elevation data, *Photogramm. Eng. Remote Sens.*, *72*, 299–311.
- Smith, T., K. Boto, and S. Frusher (1991), Keystone species and mangrove forest dynamics: The influence of burrowing by crabs on soil nutrient status and forest productivity, *Estuarine Coastal Shelf Sci.*, *33*, 419–432.
- Smith, T., M. Robblee, H. Wanless, and T. Doyle (1994), Mangroves, hurricanes, and lightning strikes, *BioScience*, *44*, 256–262.
- Smith, T. J., G. H. Anderson, K. Balentine, G. Tiling, G. A. Ward, and K. R. T. Whelan (2009), Cumulative impacts of hurricanes on Florida mangrove ecosystems: Sediment deposition, storm surges and vegetation, *Wetlands*, *29*, 24–34, doi:10.1672/08-40.1.
- Smoak, J., J. Breithaupt III, T. Smith, and C. Sanders (2013), Sediment accretion and organic carbon burial relative to sea-level rise and storm events in two mangrove forests in Everglades National Park, *Catena*, *104*, 58–66, doi:10.1016/j.catena.2012.10.009.
- Spalding, M. D., M. Kainuma, and L. Collins (2010), *World Atlas of Mangroves*, Earthscan, London, U. K.
- Suárez-Abelenda, M., T. O. Ferreira, M. Camps-Arbestain, V. H. Rivera-Monroy, F. Macías, G. N. Nóbrega, and X. L. Otero (2014), The effect of nutrient-rich effluents from shrimp farming on mangrove soil carbon storage and geochemistry under semi-arid climate conditions in northern Brazil, *Geoderma*, *213*, 551–559, doi:10.1016/j.geoderma.2013.08.007.
- Ullman, R., V. Bilbao-Bastida, and G. Grimsditch (2012), Including blue carbon in climate market mechanisms, *Ocean Coastal Manage.*, *83*, 15–18, doi:10.1016/j.ocecoaman.2012.02.009.
- Walters, B. B., P. Rönnbäck, J. M. Kovacs, B. Crona, S. A. Hussain, R. Badola, J. H. Primavera, E. Barbier, and F. Dahdouh-Guebas (2008), Ethnobiology, socio-economics and management of mangrove forests: A review, *Aquat. Bot.*, *89*, 220–236, doi:10.1016/j.aquabot.2008.02.009.
- Whelan, K. R. T., T. J. Smith, D. R. Cahoon, J. C. Lynch, and G. H. Anderson (2005), Groundwater control of mangrove surface elevation: Shrink and swell varies with soil depth, *Estuaries*, *28*, 833–843.
- Whelan, K. R. T., T. J. Smith, G. H. Anderson, and M. L. Ouellette (2009), Hurricane Wilma's impact on overall soil elevation and zones within the soil profile in a mangrove forest, *Wetlands*, *29*, 16–23, doi:10.1672/08-125.1.
- Woodroffe, C. D. (1990), The impact of sea-level rise on mangrove shorelines, *Prog. Phys. Geogr.*, *14*, 483–520, doi:10.1177/030913339001400404.
- Zimmerman, A., and E. A. Canuel (2000), A geochemical record of eutrophication and anoxia in Chesapeake Bay sediments: Anthropogenic influence on organic matter composition, *Mar. Chem.*, *69*, 117–137.